Eur. Phys. J. B **1**, 233–244 (1998)

THE EUROPEAN PHYSICAL JOURNAL B

Adsorption and spreading of polymers at plane interfaces; theory and molecular dynamics simulations

M.C.P. van Eijk[1,a], M.A. Cohen Stuart[1], S. Rovillard[2] and J. De Coninck[2]

[1] Wageningen Agricultural University, Laboratory for Physical Chemistry and Colloid Science, Dreijenplein 6, 6703 HB Wageningen, The Netherlands
[2] University of Mons-Hainaut, Research Centre for Molecular Modelling, 20 Place du Parc, 7000 Mons, Belgium

Received: 18 July 1997 / Received in final form: 27 October 1997 / Accepted: 6 November 1997

Abstract. Nonequilibrium processes play a key role in the adsorption kinetics of macromolecules. It is expected that the competition between transport of polymer towards an interface and its subsequent spreading has a significant influence on the adsorbed amount. An increase of the transport rate can lead to an increase of the adsorbed amount, especially when the polymer has too little time to spread at the interface. In this study we present both molecular dynamics simulations and analytical calculations to describe some aspects of the adsorption kinetics. From MD simulations on a poly(ethylene oxide) chain in vacuum near a graphite surface, we conclude that the spreading process can, in first approximation, be described by either a simple exponential function or by first-order reaction kinetics. Combining these spreading models with the transport equations for two different geometries (stagnation-point flow and overflowing cylinder) we are able to derive analytical equations for the adsorption kinetics of polymers at solid–liquid and at liquid–fluid interfaces.

PACS. 68.10.Jy Kinetics (evaporation, adsorption, condensation, catlysis, etc.) – 68.45.Da Adsorption and desorption kinetics; evaporation and condensation – 36.20.Ey Conformation (statistics and dynamics)

1 Introduction

The adsorption process of polymers frequently involves long-lived nonequilibrium states. The equilibrium structure of a polymer layer, as described by numerous statistical theories (see, *e.g.*, Ref. [1]), is insufficient to describe various effects observed in adsorption kinetics and statics. Several experimental studies report significant nonequilibrium processes in polymer adsorption [2–5]. One of the important parameters in the surface relaxation is the strength of the polymer–surface interaction. If the interaction energy of a single polymer segment with the interface exceeds $1kT$, then thermal fluctuations are not able to *release* parts of the polymer easily, which is necessary for its spreading. Polymers adsorbed from organic solvents on mineral surfaces interact by strong hydrogen bonds, and are therefore likely to form long-living nonequilibrium states.

Such a system was studied by Schneider *et al.* [4]. From their adsorption experiments with poly(methyl methacrylate) on silica from CCl_4 they concluded that as long as the surface coverage is low, arriving polymers will flatten and a relatively large number of polymer–surface contacts will be achieved, whereas molecules arriving at a later stage in the adsorption process will adsorb with a low bound fraction. This nonequilibrium situation turned out to be quite stable. This observation implies that polymer flux towards an interface together with the time dependent adsorbed amount $\Gamma(t)$ should have an effect on the state in which a polymer adsorbs. A slow spreading process will initially lead to a relatively small area per molecule, and thus to a relatively high adsorbed amount. Subsequent relaxation by spreading leads to an increased area per molecule, which is only possible when it is accompanied by a desorption process. This delayed spreading will lead to a decrease of $\Gamma(t)$. In this scenario a maximum (*overshoot*) in the adsorption curve will be found.

Overshoots have indeed been observed in a number of cases, both for proteins [6,5] and for synthetic polymers [2–4]. In addition, spreading plays a role in polymer–polymer exchange processes [7]. As yet, very little is known about the factors controlling the rate of the spreading process. Moreover, apart from a scaling calculation in a recent paper by Semenov and Joanny [8], the consequences of spreading for the overall adsorption kinetics have hardly been investigated.

In this paper two cases are considered: adsorption from flowing solution onto a solid surface, and adsorption onto an expanding liquid-gas or liquid–liquid interface.

[a] e-mail: mars@fenk.wau.nl

In the latter case, the rate of expansion of the interface enters the problem as a additional timescale. Pefferkorn and Elaissari [2] have introduced the *growing disk* model. In this model, each molecule is described as a disk with initial radius $S(0)$ that arrives at the interface. Immediately after attachment, the disk starts to grow exponentially with a growth rate characterized by a spreading time τ and a limiting size $S(\mathrm{eq})$. We already successfully applied an analytical version of this model to the adsorption of savinase on SiO_2 [5]. It should be important to see how realistic the growing disk model is. To this end we carried out molecular dynamics simulations on individual chains near a solid surface. We divided this study into two parts. In the first one, we introduce the relevant transport and spreading processes and also explore the latter at its molecular level. Secondly, we present analytical calculations based on the *growing disk* approach together with the two geometries in order to describe adsorption processes where spreading occurs on experimental timescales. Special attention is paid to two different spreading models.

2 Transport and spreading

The adsorption kinetics of polymers can conveniently be subdivided into three stages. Firstly, a polymer has to reach the interface by, *e.g.*, convection or diffusion. For this, the fluid dynamics of the studied system are of major importance. Secondly, an attachment of the polymer to the interface has to occur. Here several kinds of interactions may play a role, such as electrostatic or hydrophobic ones. Finally, a spreading of the molecule at the interface will occur. This spreading process will be governed by the gain or loss in the number of interaction sites between polymer and interface. Especially the characteristic times of the first and the last step in the adsorption process are of great importance for the final kinetics. Pefferkorn and Elaissari [2] applied a "growing disk" model to the adsorption kinetics of polyelectrolytes at a solid surface. They used numerical calculations to arrive at their final results. Here, we will discuss an analytical version of a comparable model, but we will also introduce a more general n-state model to address adsorption kinetics.

In the following, we will present the transport process for the case of two widely used experimental setups. Subsequently we will concentrate on two spreading models that will be used in the description of adsorption kinetics of macromolecules. We have applied molecular dynamics simulations to elucidate the spreading behaviour. These simulations justify our spreading models.

2.1 Transport to the interface

The first step in trying to describe the adsorption kinetics of polymers is deriving expressions for the transport of the molecules to the interface. In order to keep the equations relatively simple, it is necessary to work with well-defined geometries for which fluid-dynamical relations can be derived easily. In the following, we will first discuss adsorption from solution to a solid surface in a stagnation-point flow (for a rigourous fluid-dynamical approach see Ref. [9]). This setup gained much interest in reflectometric studies on polymer adsorption. A description of this technique in combination with a stagnation-point flow is given by Dijt *et al.* [10,11]. Another widely used setup which will be treated is the overflowing cylinder. This geometry is used for studying the adsorption of, *e.g.*, proteins at an air-water interface. The fluid dynamics of this geometry are described by Bergink-Martens *et al.* [12].

2.1.1 Stagnation-point flow

Figure 1 shows a schematic representation of a stagnation-point flow. The axial symmetry in the problem makes the use of cylindrical coordinates obvious. The radius of the tube is denoted by R and the distance between the outlet of the tube and the plane is given by h. We choose the stagnation-point (*i.e.*, where the fluid velocity $\mathbf{v} = \mathbf{0}$) as the origin of our coordinate system, where r denotes the radial direction, z the direction along the symmetry axis into the fluid, and ϕ the rotation around this axis. Dąbroś and Van de Ven [9] derived the following expressions for the three components of the velocity near the stagnation point for an incompressible Newtonian fluid (in dimensionless form):

$$v_r = \hat{\alpha} z r \tag{2.1a}$$

$$v_z = -\hat{\alpha} z^2 \tag{2.1b}$$

$$v_\phi = 0, \tag{2.1c}$$

where $\hat{\alpha}$ is a dimensionless flow intensity parameter depending on the Reynolds number Re and the ratio h/R. The distances r and z are made dimensionless with respect to R, and the velocity $\mathbf{v}$ with respect to the average fluid velocity U at $z = h/R$. We will use this flow field near the stagnation point for the solution of the convective diffusion equations for the transport of polymer to the interface. As flow intensity parameter we will use α which is defined as $\alpha = \hat{\alpha} U/R^2$, retaining the appropriate dimensions for the variables.

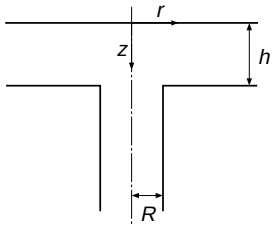

Fig. 1. Geometry of a stagnation-point flow setup. Fluid moves along the axes of symmetry in a tube of radius R and enters between two planes distance h apart. The stagnation point is the origin of a cylindrical coordinate system r, z, and ϕ (not shown).

Using conservation of mass, we write for the transport of solute i

$$\frac{\partial c_i}{\partial t} = -\nabla \cdot \mathbf{J}_i, \tag{2.2}$$

where $\mathbf{J}_i$ is the net flux and c_i the concentration of the solute (polymer). In the mentioned stagnation-point flow, diffusion and convection determine the flux. Due to the axial symmetry of the system only the r and z-components of the flux are non-zero and are given by

$$J_{ri} = c_i v_r - D_i \frac{\partial c_i}{\partial r}, \tag{2.3a}$$

$$J_{zi} = c_i v_z - D_i \frac{\partial c_i}{\partial z}, \tag{2.3b}$$

where D_i is the diffusion coefficient for component i. It must be noted that these equations are valid only under the assumption that hydrodynamic interactions are cancelled by the specific interactions between the interface and the solute [13] (Smoluchowski-Levich approximation). If we neglect radial diffusion (*i.e.*, $D_i \partial c_i/\partial r \ll c_i v_r$) then substitution of these equations in equation (2.2), where we take $\nabla \cdot \mathbf{v} = 0$ because of the incompressibility constraint, gives for the stationary state

$$\frac{\partial}{r\partial r}(r c_i v_r) + \frac{\partial c_i v_z}{\partial z} = D_i \frac{\partial^2 c_i}{\partial z^2}\,. \tag{2.4}$$

Substituting equation (2.1) into this equation gives us

$$\alpha r z \frac{\partial c_i}{\partial r} - \alpha z^2 \frac{\partial c_i}{\partial z} = D_i \frac{\partial^2 c_i}{\partial z^2}\,. \tag{2.5}$$

Symmetry implies that $\partial c_i/\partial r = 0$ at the stagnation point, thus for $r = 0$ we rewrite equation (2.5) as the linear differential equation

$$-\alpha z^2 \frac{\partial c_i}{\partial z} = D_i \frac{\partial^2 c_i}{\partial z^2}\,. \tag{2.6}$$

We are now able to derive an analytic expression for the flux J_{zi} at the stagnation point. The solution of equation (2.6) is

$$\frac{\partial c_i}{\partial z} = K_i \mathrm{e}^{-\frac{\alpha z^3}{3D_i}}. \tag{2.7}$$

The constant K_i can be found by noticing that c_i must be equal to the bulk concentration far away from the interface and c_i^0 to that in the vicinity of the interface. This subsurface concentration can in principle be found by assuming local equilibrium, implying a direct relationship between the adsorbed amount and c_i^0. We write

$$\int_0^\infty \mathrm{d}z\, \frac{\partial c_i}{\partial z} = c_i^{\mathrm{b}} - c_i^0, \tag{2.8}$$

from which we can calculate

$$K_i = \frac{(c_i^{\mathrm{b}} - c_i^0)}{\Gamma\left(\frac{1}{3}\right)} \left(\frac{9\alpha}{D_i}\right)^{1/3}, \tag{2.9}$$

where $\Gamma(x) = \int_0^\infty \mathrm{d}t\, \mathrm{e}^{-t} t^{x-1}$ denotes the Gamma function. The flux of polymer i towards the stagnation point is now given by

$$\begin{aligned} J_{zi}(0) &= D_i \left.\frac{\partial c_i}{\partial z}\right|_{z=0} \\ &= \frac{(c_i^{\mathrm{b}} - c_i^0) D_i^{2/3} (9\alpha)^{1/3}}{\Gamma\left(\frac{1}{3}\right)}. \end{aligned} \tag{2.10}$$

We will also use the limiting flux J_{0i}, which is defined as the flux $J_{zi}(0)$ for the situation where $c_i^0 = 0$.

2.1.2 Overflowing cylinder

A schematic representation of the overflowing cylinder is given in Figure 2. In this setup, again, a stagnation point exists. We choose this as the origin of our cylindrical coordinate system. In contrast to the stagnation-point flow discussed above, we are now dealing with an *expanding* interface, which introduces a new timescale. Bergink-Martens *et al.* [12] showed that if $r \ll R$, the relative expansion rate of the surface $\vartheta = \mathrm{d}A/(A\,\mathrm{d}t)$ is constant. The fluid velocities near the stagnation point are given by

$$v_r = \frac{\vartheta r}{2}, \tag{2.11a}$$

$$v_z = -\vartheta z, \tag{2.11b}$$

$$v_\phi = 0. \tag{2.11c}$$

The equations that describe the flux have already been discussed; again equations (2.2–2.4) can be used to obtain an expression for the flux towards the interface in the vicinity of the stagnation point. We substitute equation (2.11) into equation (2.4) to arrive at

$$\frac{\vartheta r}{2} \frac{\partial c_i}{\partial r} - \vartheta z \frac{\partial c_i}{\partial z} = D_i \frac{\partial^2 c_i}{\partial z^2}. \tag{2.12}$$

Symmetry implies that $\partial c_i/\partial r$ is zero at the stagnation point and negligible in its neighbourhood. Equation (2.12)

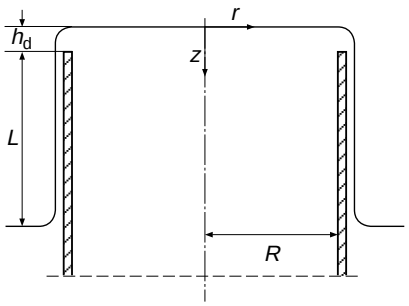

Fig. 2. Geometry of an overflowing cylinder. Fluid moves upwards in a cylinder of radius R, which will overflow, giving rise to a free expanding surface. The height L of the falling film together with the flow rate Q determine the relative expansion rate $\vartheta = \mathrm{d}A/(A\,\mathrm{d}t)$. Again, the stagnation point is the origin of a cylindrical coordinate system r, z, and ϕ (not shown).

then simplifies to

$$-\vartheta z\frac{\partial c_i}{\partial z} = D_i\frac{\partial^2 c_i}{\partial z^2}, \tag{2.13}$$

which is easily solved to obtain

$$\frac{\partial c_i}{\partial z} = K_i \mathrm{e}^{-\frac{\vartheta z^2}{2D_i}}. \tag{2.14}$$

We use the boundary condition given by equation (2.8) and obtain an expression for the integration constant

$$K_i = (c_i^{\mathrm{b}} - c_i^0)\left(\frac{2\vartheta}{D_i\pi}\right)^{12}. \tag{2.15}$$

With this equation we calculate the flux of solute i towards the interface at the stagnation point

$$\begin{aligned} J_{zi}(0) &= D_i\frac{\partial c_i}{\partial z}\bigg|_{z=0} \\ &= (c_i^{\mathrm{b}} - c_i^0)\left(\frac{2\vartheta D_i}{\pi}\right)^{1/2}. \end{aligned} \tag{2.16}$$

Again, J_{0i} will be used to express the limiting flux for $c_i^0 = 0$. The main difference of the flux between a stagnation-point flow and an overflowing cylinder setup is the different dependence on the diffusion coefficient ($D_i^{2/3}$ *vs.* $D_i^{1/2}$).

2.2 Spreading models

We are now able to describe the transport of a polymer towards an interface, but are still left with the problem of rearrangements after attachment. We will model this process as a spreading of polymer molecules at the interface. First, we will describe the rather crude, but useful, *growing disk* model, which was also used by Pefferkorn and Elaissari to model polymer adsorption kinetics [2]. Subsequently, we will discuss a simple n-step model based on first-order reaction kinetics.

In the *growing disk* model we assume that a polymer attaches to the interface in a coil conformation ($\mathcal{C}$) comparable to that in solution. After attachment the polymer will spread to its final conformation, denoted by $\mathcal{S}$. The process is then given by

$$\mathcal{C} \xrightarrow{\text{growing disk}} \mathcal{S}. \tag{2.17}$$

We take a simple exponential function for this spreading process, such that the area occupied by a polymer attached at time t' is given by

$$s(t-t') = s_{\mathrm{c}} + (s_{\mathrm{s}} - s_{\mathrm{c}})\left(1 - \mathrm{e}^{-\frac{t-t'}{\tau_{\mathrm{s}}}}\right), \tag{2.18}$$

where s_{c} and s_{s} are the initial and final occupied area of the molecule per unit mass, respectively.

A discrete form of the *growing disk* model is obtained if we assume that the polymer can be present at the interface in $n+1$ different conformations. Schematically the spreading process can then be depicted as

$$\mathcal{P}_0 \underset{k_{-1}}{\overset{k_{+1}}{\rightleftarrows}} \mathcal{P}_1 \;\cdots\; \mathcal{P}_{n-1} \underset{k_{-n}}{\overset{k_{+n}}{\rightleftarrows}} \mathcal{P}_n, \tag{2.19}$$

where k_{+i} and k_{-i} are reaction rate constants for the surface processes. The areas per unit mass for the $n+1$ states are denoted by s_i. We can simply apply first-order reaction kinetics to calculate the adsorbed amounts of the different conformations. There also exists a direct relation between the adsorbed amounts and the surface coverage θ:

$$\theta = \sum_{i=0}^{n} \Gamma_i s_i. \tag{2.20}$$

In practice it is useful to use the one-step version of this model, defining $k_{\mathrm{f}} \equiv k_{+1}$ and $k_{\mathrm{b}} \equiv k_{-1}$ as reaction rate constants, and take s_{c} and s_{s} as the area of the polymer in the initial and final state, respectively.

2.3 Molecular dynamics

Before proceeding to an analytical description of the adsorption kinetics of spreading polymers, we would like to give a possible justification on a molecular level for the introduced spreading models. To this end, we carried out some molecular dynamics simulation on a fairly simple model system, from which we are able to extract the spreading behaviour near a solid surface.

2.3.1 Model system and procedure

One of the aspects to keep in mind when trying to simulate the spreading of a polymer near an interface, is the accessible timescale. It should be clear that we should pick a model system where spreading will be fast, and as a consequence we have to limit ourselves to relatively small flexible molecules at a very low density.

The systems we studied all consist of a single chain of poly(ethylene oxide) (PEO) with protons as end groups near a graphite surface. We will denote these polymers as EO_n, where n is the number of ethylene oxide groups. The graphite surface is a single layer consisting of 1881 C-atoms. All simulations on the PEO system were carried out using the commercially available software Insight II 4.0.0 from MSI together with the Discover 96.0/4.0.0 module. To get reliable results on the spreading behaviour of PEO, each simulation was build up in four stages. Before going in these details, we first mention some characteristics of the MD simulation.

The microscopic state of a system of N atoms can be described in terms of the positions ($\mathbf{r}_i$) and momenta ($\mathbf{p}_i$) of the contained atoms. To characterize the system we will use a convenient condensed notation

$$\mathbf{r} = (\mathbf{r}_1, \mathbf{r}_2, \ldots, \mathbf{r}_N) \tag{2.21a}$$

$$\mathbf{p} = (\mathbf{p}_1, \mathbf{p}_2, \ldots, \mathbf{p}_N). \tag{2.21b}$$

As is common, we write the Hamiltonian of the system as a sum of potential and kinetic energy terms:

$$\mathcal{H}(\mathbf{r},\mathbf{p}) = \mathcal{V}(\mathbf{r}) + \mathcal{K}(\mathbf{p}). \tag{2.22}$$

We use the consistent valence force field from the Discover module without cross terms arriving at the following expression for the potential energy contribution to the Hamiltonian:

$$\begin{aligned}\mathcal{V}(\mathbf{r}) = &\sum_i k_{bi}\left(b_i - b_i^0\right)^2 + \sum_i k_{\theta i}\left(\theta_i - \theta_i^0\right)^2 \\ &+ \sum_i k_{\phi i}\left(1 + \cos\left(n\phi_i - \phi_i^0\right)\right) \\ &+ \sum_i k_{\chi i}\left(1 + \cos\left(n\chi_i - \chi_i^0\right)\right) \\ &+ \sum_{ij}\left(\left(\frac{A_{ij}}{r_{ij}}\right)^{12} - \left(\frac{B_{ij}}{r_{ij}}\right)^{6}\right) + \sum_{ij}\frac{q_i q_j}{4\pi\epsilon r_{ij}},\end{aligned} \tag{2.23}$$

where b_i is a bond length, θ_i a bond angle, ϕ_i a torsion angle, χ_i an out-of-plane angle to correct for torsional bonds $\phi_i \approx \pi$ in the case of π-bonds (cis-conformation), and q_i the charge of an atom. The distance between atom i and j is denoted by r_{ij}. All other symbols denote constants depending on the kind of concerned atoms, which define the force field. The Lennard-Jones potential is calculated only to a cut-off radius $r_{ij} = 2.5$ nm, and the electrostatic contribution to a cut-off radius $r_{ij} = 0.95$ nm.

In our MD simulations we imply effectively no boundary conditions, allowing the polymer to move freely in vacuum. At the beginning, the system is arranged so that the centre of mass ($\mathbf{R}_{\mathrm{cm}}$) of the PEO molecule is at a distance of 5 nm from the graphite sheet plane. We choose the origin of a Cartesian coordinate system to be in the graphite plane and the z-direction perpendicular to it. To save computational time, the carbon atoms in the graphite layer are held fixed to their initial positions during all steps of the simulation. However, they will contribute to the non-bond terms of the potential energy in their interactions with the PEO.

Having situated the PEO molecule far from the surface we perform a potential energy minimization to equilibrate the polymer structure. For this purpose we use a cascade of two minimisers, starting with the steepest-descent method, followed by the conjugate-gradient one. The steepest-descent algorithm is used to make sure that any severe strain within the polymer chain is removed. We apply this method until the gradient of the potential energy with respect to the atom coordinates $|\nabla_{\mathbf{r}}\mathcal{V}(\mathbf{r})| \leq 4.184 \times 10^{16}\,\mathrm{J\,mol^{-1}m^{-1}}$. We then proceed with the conjugate-gradient method until $|\nabla_{\mathbf{r}}\mathcal{V}(\mathbf{r})| \leq 4.184\times10^{10}\,\mathrm{J\,mol^{-1}m^{-1}}$. After this minimization step the PEO molecule has adopted a structure close to a local potential energy minimum.

In the presence of a fully minimized configuration of PEO, we can start the molecular dynamics simulation with a target temperature $T = 298$ K in a NVT ensemble. To force the polymer towards the surface, we apply a constraint to the centre of mass of the PEO. So, in the potential energy an extra term

$$v_{\mathrm{cm}} = k(z_{\mathrm{cm}} - z_0)^2 \tag{2.24}$$

occurs, with $k = 2.092\times10^{27}\,\mathrm{J\,mol^{-1}m^{-1}}$ and $z_0 = 2.5$ nm. This quadratic potential is used during the first 10000 steps of 1 fs of our simulation. The polymer is than close enough to the surface to start our final step in the MD simulation.

Before the adsorption and spreading stage, we replace the previously introduced quadratic constrained by a flat-bottomed constraint

$$v_{\mathrm{cm}} = \begin{cases} k(z_{\mathrm{cm}} - z_0)^2 & \text{for } z_{\mathrm{cm}} < z_0, \\ 0 & \text{for } z_0 \leq z_{\mathrm{cm}} \leq z_1, \\ k(z_{\mathrm{cm}} - z_1)^2 & \text{for } z_{\mathrm{cm}} > z_1, \end{cases} \tag{2.25}$$

where $z_0 = 0$ nm, $z_1 = 2.5$ nm, and $k = 4.184 \times 10^{12}$ J mol^{-1}m^{-1}. This restraint prevents the PEO from moving too far from the graphite surface without influencing its behaviour in the vicinity of the surface. We run the MD simulation over 60000 time steps of 1 fs. Every 10 fs all atom coordinates are stored for post-processing.

In our simulations we varied the chain length ($n = 10, 30, 50$) and the interaction between PEO and the graphite sheet. The latter is achieved by scaling the Lennard-Jones potential between polymer atoms and graphite atoms by a factor γ.

From the stored atom positions of PEO, taken from $\mathbf{r}$ every 10 fs, we calculated a number of relevant quantities in order to visualize the adsorption and spreading process. The position of the polymer is reflected in the position of the centre of mass which is defined as

$$\mathbf{R}_{\mathrm{cm}} \equiv \frac{\sum_{i=1}^{N_{\mathrm{p}}} m_i \mathbf{r}_i}{\sum_{i=1}^{N_{\mathrm{p}}} m_i}, \tag{2.26}$$

where m_i is the mass of atom i and N_{p} is the number of atoms in the PEO molecule. This $\mathbf{R}_{\mathrm{cm}}$ can subsequently be used to calculate a mean distance of the PEO molecule to the surface

$$z_{\mathrm{cm}} = \mathbf{R}_{\mathrm{cm}} \cdot \mathbf{e}_z, \tag{2.27}$$

where $\mathbf{e}_z$ is the unit vector in the z-direction of the Cartesian coordinate system. The spreading process can be monitored by following the evolution of the parallel radius of gyration of PEO, defined as

$$R_{\mathrm{g}\parallel}^2 \equiv \frac{\sum_{i=1}^{N_{\mathrm{p}}} m_i \left((\mathbf{r}_i - \mathbf{R}_{\mathrm{cm}})^2 - ((\mathbf{r}_i - \mathbf{R}_{\mathrm{cm}}) \cdot \mathbf{e}_z)^2\right)}{\sum_{i=1}^{N_{\mathrm{p}}} m_i}. \tag{2.28}$$

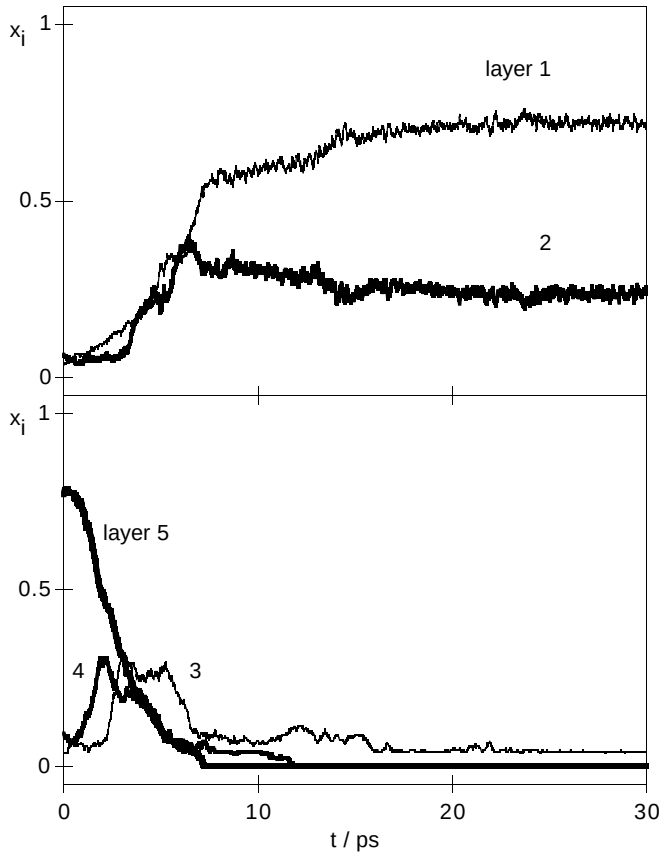

Fig. 3. Fraction x_i of the atoms of EO_{30} in a 0.5 nm thick layer i ($i = 1, 2, 3, 4, 5$) parallel to the surface. The layers are numbered from the surface.

Furthermore, the distribution of the PEO atoms perpendicular to the surface is calculated. To this end, the number of atoms N_i in layer i of 0.5 nm in thickness, parallel to the surface, are counted for 5 layers. The fraction of atoms in layer i is then denoted by $x_i = N_i/N_\mathrm{p}$.

2.3.2 MD Results

As an example of the observed effects for the adsorption and spreading of PEO on a graphite surface, we will illustrate here the results obtained for EO_{30} with $\gamma = 3$. Similar results were also found for the other studied systems. At the start of the MD simulation the PEO is approximately 2.5 nm from the surface, and has to approach it, before a polymer segment will be in contact with the graphite. How this happens is depicted in Figure 3, where the fraction of the EO_{30} that is present in a layer at a certain distance from the surface is plotted as function of time. Clearly, the polymer starts from layer 5 (2.0–2.5 nm from the surface), and subsequently adsorbs and mainly ends up in layers 1 and 2. This implies a rather flat conformation of the molecule in the adsorbed state. This observation confirms the existence of a spreading process. The approach towards the surface can also be nicely monitored by the time dependence of the vertical position of the centre of mass as defined by equation (2.27), which is shown in Figure 4. From this plot, however, we are not able to draw satisfying conclusions about the time constant of the spreading process. A more suitable quantity for this purpose is the radius of gyration of the PEO parallel to the surface.

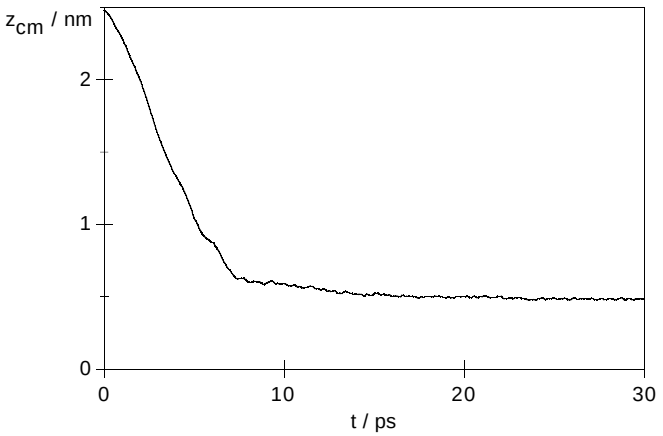

Fig. 4. Approach of the centre of mass of EO_{30} to the graphite surface in the final stage of the MD simulation.

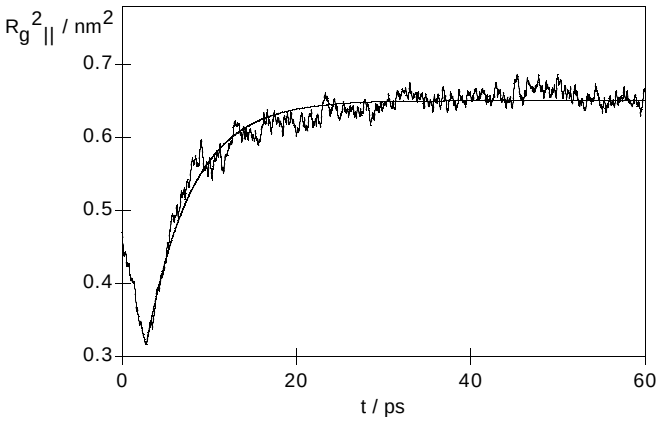

Fig. 5. $R^2_{\mathrm{g}\parallel}$ as a measure for the occupied area of EO_{30} as a function of time. Also shown is a fit of the data to the function $R^2_{\mathrm{g}\parallel} = R^2_{\mathrm{g}0} + \sigma\left(1 - \exp\left(-\frac{t-t_0}{\tau}\right)\right)$.

Figure 5 shows the time evolution of $R^2_{\mathrm{g}\parallel}$ for EO_{30}. The fact that the parallel size of the PEO decreases in the beginning of the simulation is caused by the fact that at that point the polymer is pulled towards the surface after release of the constraint in the potential energy from equation (2.24). The spreading of the polymer is clearly seen, and in order to compare it to our introduced spreading models in the previous section (Eq. (2.18)) we fitted the data to the following equation:

$$R^2_{\mathrm{g}\parallel} = R^2_{\mathrm{g}0} + \sigma\left(1 - \exp\left(-\frac{t - t_0}{\tau}\right)\right), \qquad (2.29)$$

with $R^2_{\mathrm{g}0} = 0.316$ nm^2, $\sigma = 0.334$ nm^2, $t_0 = 2.82$ ps, and $\tau = 5.18$ ps. In this fit t_0 and $R^2_{\mathrm{g}0}$ are taken from the data by hand. Comparison of this fit with the data suggests that a simple exponential function is a good first approximation for the spreading of a flexible polymer near an interface.

One should bear in mind that the presented simulation only serves as an example, and that similar behaviour was observed for the other simulation runs. It should be evident that the presence of more polymers will complicate the situation. However, as long as the surface coverage is relatively low the single polymer approach serves as a good first approximation. For now we will use this crude model in our analytical calculations.

3 Analytical expressions for adsorption kinetics

In this section we will combine the above introduced transport equations and spreading models to arrive at analytical equations for the adsorption kinetics of macromolecules.

3.1 Adsorption at immobile interfaces

One of the most common interfaces for the adsorption of polymers is a solid–liquid one. In this case no convective polymer transport along the interface can occur. We will discuss the adsorption in a stagnation-point flow on such an immobile interface. If we assume that the attachment of polymer to the interface is fast as compared to the transport, then the adsorption rate is equal to the polymer flux J. So for the total adsorbed amount we write

$$\frac{\mathrm{d}\Gamma}{\mathrm{d}t} = J = J_0 \frac{c^{\mathrm{b}} - c^0}{c^{\mathrm{b}}}. \tag{3.1}$$

The limiting flux J_0 is given by equation (2.10), where we take $c_0 = 0$. Because the calculation of c_0 requires a non-trivial molecular model for the adsorption process, we will introduce a rather simplified model for the adsorption rate. We assume that the adsorption rate is proportional to the free surface area and the limiting polymer flux, giving

$$\frac{\mathrm{d}\Gamma}{\mathrm{d}t} = J_0 \beta, \tag{3.2}$$

where the relative free surface area is denoted as $\beta = 1-\theta$. We realize that, using this assumption, we underestimate the adsorption rate, but it is a convenient first-order approximation which still allows us to predict the correct trends.

To take surface processes of the polymer into account, we will apply the two discussed spreading models to derive equations for the adsorbed amount.

3.1.1 Growing disk

When using the *growing disk* model it is most convenient the derive an equation for the relative free surface area β, which can be used to solve equation (3.2). An amount $\mathrm{d}\Gamma$ adsorbed during a time interval $\mathrm{d}t'$ will occupy a fraction $\mathrm{d}\theta$ of the surface at time t given by

$$\mathrm{d}\theta = J_0 \beta(t') s(t-t') \mathrm{d}t'. \tag{3.3}$$

The occupied area $s(t-t')$ is taken from equation (2.18). Before continuing it is convenient to non-dimensionalize all variables by the following rescaling:

$$J_0 s_{\mathrm{c}} \tau_{\mathrm{s}} \to J, \quad \Gamma s_{\mathrm{c}} \to \Gamma, \quad s_{\mathrm{s}}/s_{\mathrm{c}} \to \sigma, \quad t/\tau_{\mathrm{s}} \to t. \tag{3.4}$$

We obtain the relative free surface area by assuming an empty surface at $t = 0$, and calculating the fraction of occupied surface by integrating equation (3.3). We then arrive at

$$\beta(t) = 1 - J \int_0^t \mathrm{d}t' \, \beta(t') \left(1 + (\sigma - 1)\left(1 - \mathrm{e}^{t'-t}\right)\right). \tag{3.5}$$

This integral equation can be transformed to a differential equation by differentiating twice. After some rewriting we arrive at

$$\frac{\mathrm{d}^2\beta}{\mathrm{d}t} + (1+J)\frac{\mathrm{d}\beta}{\mathrm{d}t} + J\sigma\beta = 0. \tag{3.6}$$

The solution of this linear, homogeneous differential equation is easily derived. Appendix A.1 shows how it is done. The relevant boundary conditions of this equation are already contained in equation (3.5), they are

$$\beta(0) = 1, \quad \left.\frac{\mathrm{d}\beta}{\mathrm{d}t}\right|_{t=0} = -J. \tag{3.7}$$

Equation (3.6) has three different solutions, depending on the roots of its characteristic equation. The discriminant of this equation is given by $D = (1+J)^2 - 4J\sigma$. The relative free surface area is calculated from equation (A.2) by insertion of the boundary conditions. This leads to:

for $D > 0$

$$\beta = -\frac{1 - J - \sqrt{D}}{2\sqrt{D}} \mathrm{e}^{-\frac{1+J+\sqrt{D}}{2}t} + \frac{1 - J + \sqrt{D}}{2\sqrt{D}} \mathrm{e}^{-\frac{1+J-\sqrt{D}}{2}t}, \tag{3.8a}$$

for $D = 0$

$$\beta = \left(1 + \frac{1-J}{2}t\right) \mathrm{e}^{-\frac{1+J}{2}t}, \tag{3.8b}$$

for $D < 0$

$$\beta = \left(\cos\frac{\sqrt{-D}}{2}t + \frac{1-J}{\sqrt{-D}} \sin\frac{\sqrt{-D}}{2}t\right) \mathrm{e}^{-\frac{1+J}{2}t}. \tag{3.8c}$$

By noting that $\sqrt{-D} = i\sqrt{D}$, $\cos x = \cosh ix$, and $\sin x = -i \sinh ix$, it is easily seen that equation (3.8a) is equivalent to equation (3.8c). The adsorbed amount is now calculated by substitution of the previously obtained constants in equation (A.3):

for $D > 0$

$$\frac{\Gamma}{J} = \frac{1}{J\sigma} + \frac{1 - J - \sqrt{D}}{(1 + J + \sqrt{D})\sqrt{D}} \mathrm{e}^{-\frac{1+J+\sqrt{D}}{2}t} - \frac{1 - J + \sqrt{D}}{(1 + J - \sqrt{D})\sqrt{D}} \mathrm{e}^{-\frac{1+J-\sqrt{D}}{2}t}, \tag{3.9a}$$

for $D = 0$

$$\frac{\Gamma}{J} = \frac{1}{J\sigma} - \frac{4 + (1 - J^2)t}{(1 + J)^2} \mathrm{e}^{-\frac{1+J}{2}t}, \tag{3.9b}$$

for $D < 0$

$$\frac{\Gamma}{J} = \frac{1}{J\sigma} \left[1 - \left(\cos \frac{\sqrt{-D}}{2} t + \frac{1 - J^2 + D}{2\sqrt{-D}} \sin \frac{\sqrt{-D}}{2} t \right) \mathrm{e}^{-\frac{1+J}{2}t} \right]. \tag{3.9c}$$

3.1.2 One-step model

Instead of finding an equation for the relative free surface area, it is also possible to obtain a set of differential equations directly, where we assume that a polymer can be present at the interface in two different states. We can then treat the adsorbed amount of the polymer in the different states separately. To this end, equation (3.2) is replaced by

$$\frac{\mathrm{d}\Gamma_\mathrm{c}}{\mathrm{d}t} = J_0(1 - \Gamma_\mathrm{c} s_\mathrm{c} - \Gamma_\mathrm{s} s_\mathrm{s}) - k_\mathrm{f}\Gamma_\mathrm{c} + k_\mathrm{b}\Gamma_\mathrm{s}, \tag{3.10a}$$

$$\frac{\mathrm{d}\Gamma_\mathrm{s}}{\mathrm{d}t} = k_\mathrm{f}\Gamma_\mathrm{c} - k_\mathrm{b}\Gamma_\mathrm{s}, \tag{3.10b}$$

where the subscripts "c" and "s" refer to the coiled and spread states, respectively. The reaction constants for the forward (spreading) and backward (coiling) reaction are denoted by k_f and k_b. Again, we non-dimensionalize the equations by the rescaling

$$\frac{J_0 s_\mathrm{c}}{k_\mathrm{f}} \to J, \quad \Gamma_i s_\mathrm{c} \to \Gamma_i, \quad \frac{s_\mathrm{s}}{s_\mathrm{c}} \to \sigma, \quad \frac{k_\mathrm{b}}{k_\mathrm{f}} \to \kappa, \quad t k_\mathrm{f} \to t. \tag{3.11}$$

We write equation (3.10) in a dimensionless Einstein matrix notation

$$\dot{\Gamma}_j = A_{jk}\Gamma_k + J_j \tag{3.12}$$

with the boundary condition $\Gamma_j(0) = 0$. Appendix A.2 gives the general solutions of a set of m linear, nonhomogeneous first order differential equations. Our interest is in $m = 2$, for which the adsorbed amounts for the two states are given by

$$\Gamma_\mathrm{c} = \frac{\kappa}{\kappa + \sigma} - J\frac{1 + J - \kappa + \sqrt{D}}{\sqrt{D}(1 + J + \kappa + \sqrt{D})} \mathrm{e}^{-\frac{1+J+\kappa+\sqrt{D}}{2}t} + J\frac{1 + J - \kappa - \sqrt{D}}{\sqrt{D}(1 + J + \kappa - \sqrt{D})} \mathrm{e}^{-\frac{1+J+\kappa-\sqrt{D}}{2}t}, \tag{3.13a}$$

$$\Gamma_\mathrm{s} = \frac{1}{\kappa + \sigma} + \frac{2J}{\sqrt{D}(1 + J + \kappa + \sqrt{D})} \mathrm{e}^{-\frac{1+J+\kappa+\sqrt{D}}{2}t} - \frac{2J}{\sqrt{D}(1 + J + \kappa - \sqrt{D})} \mathrm{e}^{-\frac{1+J+\kappa-\sqrt{D}}{2}t}, \tag{3.13b}$$

where

$$D = (1 + J + \kappa)^2 - 4J(\kappa + \sigma). \tag{3.14}$$

These equations are valid only if $D \neq 0$, *i.e.*, the eigenvalues of A_{jk} are distinct. We will not give the equations for $D = 0$ here, because they are only limits of the general solution, and are therefore physically of little use. Finally, the surface coverage θ is easily calculated by substitution of equation (3.13) in $\theta = \Gamma_\mathrm{c} + \sigma\Gamma_\mathrm{s}$.

Comparing the equation for the total adsorbed amount $\Gamma = \Gamma_\mathrm{c} + \Gamma_\mathrm{s}$ with equation (3.9a) for the "growing disk" model, one observes that they are identical if we take $\kappa = 0$. This is what we expected, because the exponential function taken for the "growing disk" model is just the result of first order reaction kinetics without reverse reaction ($k_\mathrm{b} = 0$).

3.2 Adsorption at expanding interfaces

Adsorption of polymers, and especially proteins, at expanding liquid–gas interfaces is of interest in, *e.g.*, foaming processes. Again, we assume the adsorption rate to be proportional to the free surface area, but we also have to take into account the transport of polymer along the interface. Hence, the continuity equation reads

$$\frac{\mathrm{d}\Gamma}{\mathrm{d}t} = -\vartheta\Gamma + J_0\beta, \tag{3.15}$$

where it should be noted that the polymer flux J_0 is a function of the expansion rate of the interface (see Eq. (2.16)). Unfortunately, it is in this case not possible to derive a simple equation for the free surface area β, because a polymer adsorbing at t' will be at another location at the interface at time t. Calculation of the occupied area therefore requires an Eulerian approach. So, in this case it is more convenient to use the one-step model.

3.2.1 One-step model

If we assume that a polymer is in a coiled state in solution, and can be in either a coiled or a spread state at the interface, we can rewrite equation (3.15) for the adsorbed amounts of the two states as

$$\frac{\mathrm{d}\Gamma_\mathrm{c}}{\mathrm{d}t} = J_0(1 - \Gamma_\mathrm{c}s_\mathrm{c} - \Gamma_\mathrm{s}s_\mathrm{s}) - k_\mathrm{f}\Gamma_\mathrm{c} + k_\mathrm{b}\Gamma_\mathrm{s} - \vartheta\Gamma_\mathrm{c}, \tag{3.16a}$$

$$\frac{\mathrm{d}\Gamma_\mathrm{s}}{\mathrm{d}t} = k_\mathrm{f}\Gamma_\mathrm{c} - k_\mathrm{b}\Gamma_\mathrm{s} - \vartheta\Gamma_\mathrm{s}. \tag{3.16b}$$

We use the same rescaling as in equation (3.11) with the addition of $\vartheta/k_\mathrm{f} \to \vartheta$. We use the same Einstein matrix notation as in the immobile interface case:

$$\dot{\Gamma}_j = A_{jk}\Gamma_k + J_j \tag{3.17}$$

with the boundary condition $\Gamma_j(0) = 0$. The solution can thus be taken from appendix A.2. The adsorbed amounts for the two states are given by

$$\begin{aligned}\Gamma_\mathrm{c} = {} & \frac{J(\kappa+\vartheta)}{J(\kappa+\sigma)+\vartheta(1+J+\kappa+\vartheta)} \\ & - J\frac{1+J-\kappa+\sqrt{D}}{\sqrt{D}(1+J+\kappa+2\vartheta+\sqrt{D})}\mathrm{e}^{-\frac{1+J+\kappa+2\vartheta+\sqrt{D}}{2}t} \\ & + J\frac{1+J-\kappa-\sqrt{D}}{\sqrt{D}(1+J+\kappa+2\vartheta-\sqrt{D})}\mathrm{e}^{-\frac{1+J+\kappa+2\vartheta-\sqrt{D}}{2}t},\end{aligned} \tag{3.18a}$$

$$\begin{aligned}\Gamma_\mathrm{s} = {} & \frac{J}{J(\kappa+\sigma)+\vartheta(1+J+\kappa+\vartheta)} \\ & + \frac{2J}{\sqrt{D}(1+J+\kappa+2\vartheta+\sqrt{D})}\mathrm{e}^{-\frac{1+J+\kappa+2\vartheta+\sqrt{D}}{2}t} \\ & - \frac{2J}{\sqrt{D}(1+J+\kappa+2\vartheta-\sqrt{D})}\mathrm{e}^{-\frac{1+J+\kappa+2\vartheta-\sqrt{D}}{2}t},\end{aligned} \tag{3.18b}$$

where

$$D = (1+J+\kappa)^2 - 4J(\kappa+\sigma). \tag{3.19}$$

As is the case for adsorption at immobile interfaces, these equations are also valid only if $D \neq 0$, *i.e.*, the eigenvalues of A_{jk} have to be distinct. At this point it is also important to note that the fact that $J \propto c_\mathrm{p}\vartheta^{1/2}$ (see Eq. (2.16)) limits the possibility of varying ϑ and J independently.

4 Discussion and conclusion

In this section we will give some sample calculations with the presented models and discuss the validity of the models. We will especially focus on the restrictions of the models.

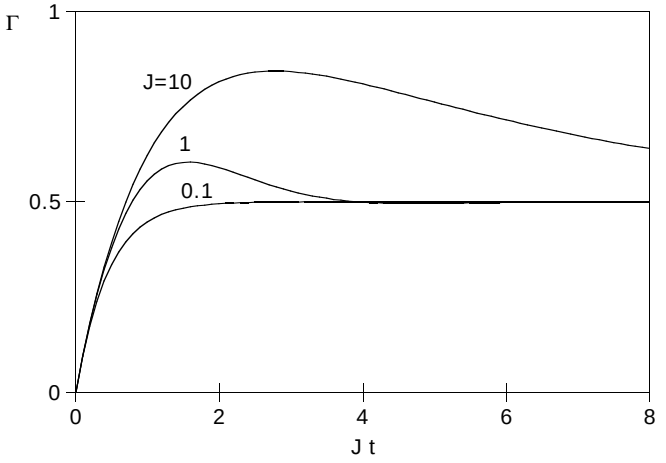

Fig. 6. Dimensionless adsorbed amount $\Gamma(Jt)$ of a spreading polymer at an immobile interface as calculated by equation (3.9) or (3.13) with $\sigma = 2$, and $\kappa = 0$. The polymer flux J is indicated in the plot.

4.1 Immobile interface

The adsorption of a spreading polymer at a solid–liquid interface is determined by two competing processes: the transport to the surface and the spreading. As an example we take the occupied area of a completely unfolded molecule to be twice that of a coiled polymer, *i.e.*, $\sigma = 2$. Figure 6 shows the time dependence of the total adsorbed amount as calculated with the one-step model (see Eq. (3.13)) for $\kappa = 0$ at different limiting polymer fluxes. The same plot is obtained by equation (3.9) for the *growing disk* model. The adsorbed amount Γ is plotted against Jt to obtain an initial slope of unity in all cases. It is easy to show that there is a threshold for J beyond which the calculated adsorbed amount has a maximum value at a finite time t_max. The desorption observed after this time is of a non-physical nature, because we allow polymers to spread on a fully occupied surface. Therefore, a negative free surface area β occurs, which can eventually even lead to a negative adsorbed amount of the coiled polymer as can be seen in Figure 7, where we plot the adsorbed amounts for each of the different states of the polymer, with $\kappa = 0$, $\sigma = 2$, and $J = 1$. This observation indicates that the equations used are only valid until t_max where $\beta = 0$ for the first time. The time t_max where this maximum is reached is calculated from $\theta = \Gamma_\mathrm{c} + \sigma\Gamma_\mathrm{s} = 1$:

$$t_\mathrm{max} = \begin{cases} \dfrac{1}{\sqrt{D}}\ln\dfrac{1-J+\kappa-\sqrt{D}}{1-J+\kappa+\sqrt{D}} \\ \qquad \text{for } J > \kappa + 2\sigma - 1, \\ \dfrac{1}{\sqrt{D}}\left(\ln\dfrac{1-J+\kappa-\sqrt{D}}{1-J+\kappa+\sqrt{D}} + 2\pi i\right) \\ \qquad \text{for } J < \kappa + 2\sigma - 1 \wedge D < 0, \\ \infty \qquad \text{in other cases.} \end{cases} \tag{4.1}$$

Substituting equation (4.1) in equation (3.13) gives the maximum adsorbed amount for both the coiled and

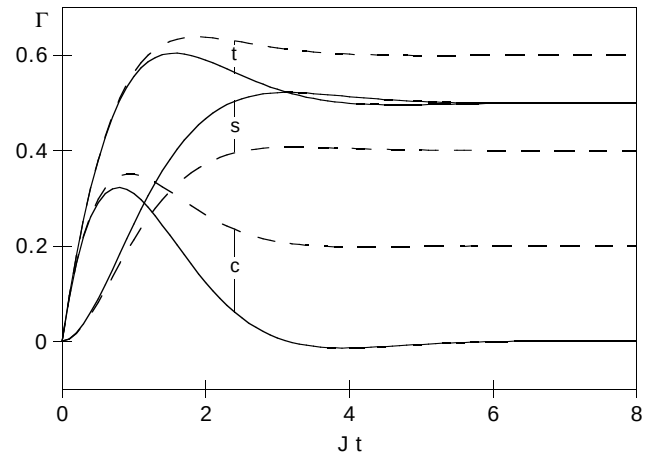

Fig. 7. Adsorbed amount of the coiled (c) and spread (s) state of a polymer at an immobile surface with $\sigma = 2$ and $J = 1$. The total adsorbed amount (t) is also plotted. Solid lines: $\kappa = 0$; dashed lines: $\kappa = 0.5$.

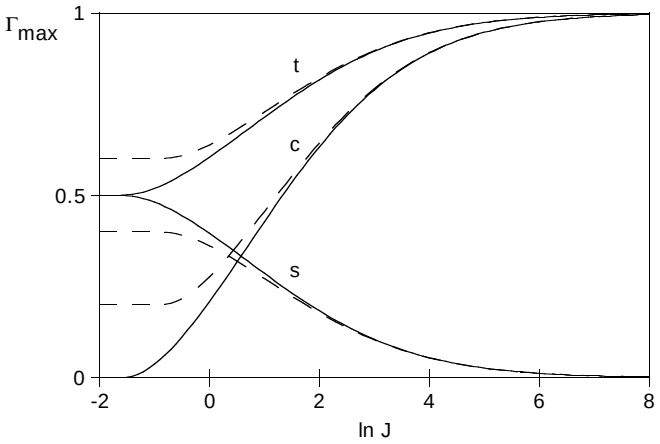

Fig. 8. Adsorbed amount at $t_{\max}$ of a spreading polymer at an immobile interface, for $\sigma = 2$. Curves are shown for the coiled state (c), the spread state (s), and the total (t). Solid lines: $\kappa = 0$; dashed lines: $\kappa = 0.5$.

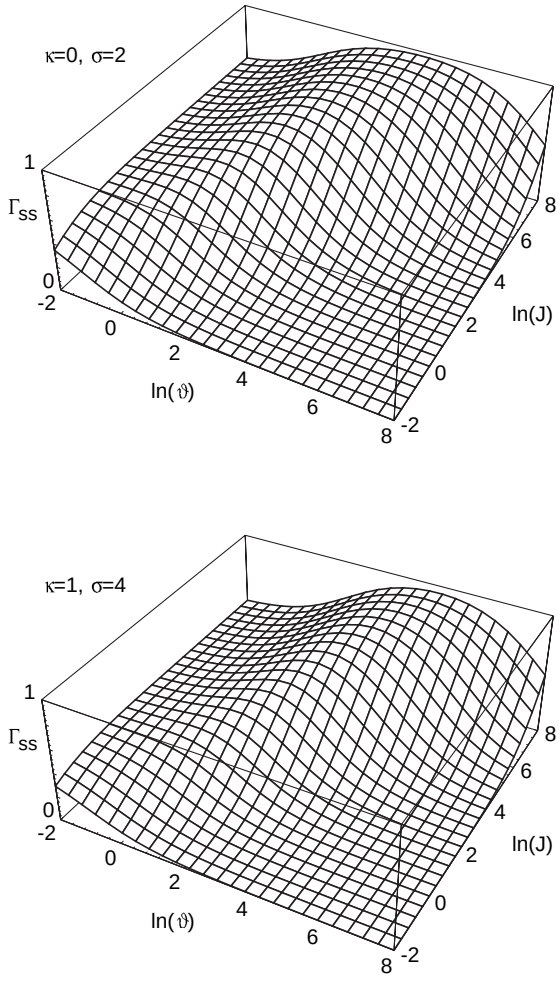

Fig. 9. Adsorbed amount in a stationary state for a polymer adsorbing at an expanding interface as a function of the surface expansion rate ϑ and the limiting polymer transport J. Upper graph: irreversible spreading ($\kappa = 0$) with $\sigma = 2$. Lower graph: reversible spreading ($\kappa = 1$) with $\sigma = 4$.

the spread state. Figure 8 gives two examples of these maximum adsorbed amounts as a function of J. It is obvious that by taking $\kappa > 0$, the final adsorbed amount of the coiled state will be larger, and therefore the occupied area smaller. This leads to an increase of the total adsorbed amount, as is seen in this figure.

From Figure 8 it is clear that the transport rate can be used to control the final mass and structure of an adsorbed polymer layer. One should however bear in mind that the experimental window may be well outside the interesting region, *i.e.*, $0 \lesssim \ln(J) \lesssim 4$. This can for instance be the case for the adsorption of flexible polymers, because then the spreading process will be too fast.

4.2 Expanding interface

The only significant difference in the case that the interface is mobile, is that forced transport of adsorbed molecules along the interface will now occur. One of the consequences of this difference is that the *overshoot* of the surface coverage θ observed in the calculations for the immobile interface, is only present for small values of ϑ, and is relatively small, *i.e.*, $1 - \theta \ll 1$. The adsorption of polymers and proteins at a liquid–air interface is often studied in a stationary state, such as obtained with the overflowing cylinder. Therefore, we will only discuss the maximum adsorbed amounts, which are independent of the boundary conditions of equation (3.17) as long as we neglect the possible overshoot mentioned above.

These maximum adsorbed amounts are easily calculated by setting $\dot{\Gamma}_j = 0$ in equation (3.17) or by taking $t \to \infty$ in equation (3.18), and are thus given by the first terms in equations (3.18a, 3.18b), respectively. The total adsorbed amount in the stationary state is thus found to be

$$\Gamma_{\rm ss} = \frac{J(1+\kappa+\vartheta)}{J(\kappa+\sigma)+\vartheta(1+J+\kappa+\vartheta)}\,. \qquad (4.2)$$

Figure 9 shows two examples of $\Gamma_{\rm ss}$ as a function of J and ϑ. Clearly, in an overflowing cylinder setup it is possible to control the amount of polymer adsorbed by changing either J (*e.g.*, by way of changing the polymer concentration) or ϑ.

4.3 Final remarks

We have shown that with a straight forward analytical approach we are able to describe the adsorption and spreading of chain molecules. In a previous paper it was shown that the presented model is indeed capable of, at least qualitatively, describing the adsorption of the protein savinase on silica [5]. The use of intrinsically simple spreading models is justified by molecular dynamics simulations of poly(ethylene oxide) near a graphite surface. The major limitations of our model are the fact that we underestimate the polymer flux towards the surface by assuming a linear dependence of this flux with the free surface area (see Eqs. (3.2) and (3.15)), and the fact that the spreading itself is independent of the surface coverage. This implies that the presented models should be used with care, and are bound to give qualitative, rather than exact quantitative, agreement with experiments.

Two of us (MvE and MCS) thank Herman van Leeuwen and Marcel Minor for useful comments and discussions. These investigations are supported by the Netherlands Foundation for Chemical Research (SON) with financial aid from the Netherlands Organisation for Scientific Research (NWO). This research is also sponsored by the EC Human and Capital Mobility programme CHRX-CT94-0448-3.

Appendix A: Differential equations in adsorption kinetics

The analysis of the adsorption kinetics of polymers involves the solution of differential equations. Here, we will give a general approach in solving such equations for two kind of spreading models for the polymer at the interface.

A.1 Growing disk

If we assume that an adsorbing polymer will change its conformation at the interface by some simple exponential function, the relative free surface area β will be given by a linear, homogeneous second-order differential equation of the following form:

$$\frac{{\rm d}^2\beta}{{\rm d}t^2} + b\frac{{\rm d}\beta}{{\rm d}t} + c\beta = 0. \tag{A.1}$$

Let m_1 and m_2 be the roots of the characteristic equation $m^2 + bm + c = 0$, and let $D = b^2 - 4c$. Then there are three cases:

$$\beta = c_1{\rm e}^{m_1 t} + c_2{\rm e}^{m_2 t} \qquad \text{for } D > 0, \tag{A.2a}$$

$$\beta = c_1{\rm e}^{m_1 t} + c_2 t{\rm e}^{m_1 t} \qquad \text{for } D = 0, \tag{A.2b}$$

$$\beta = (c_1\cos qt + c_2\sin qt){\rm e}^{pt} \qquad \text{for } D < 0, \tag{A.2c}$$

where $p = -b/2$ and $q = \sqrt{4c - b^2}/2$. The calculation of the adsorbed amount Γ involves the solution of the linear, first-order differential equation ${\rm d}\Gamma/{\rm d}t = J\beta$ (see Eq. (3.2)). The adsorbed amount is simply given by $\Gamma = J\int_0^t {\rm d}t'\,\beta$, where we assumed $\Gamma(0) = 0$, so:

for $D > 0$

$$\frac{\Gamma}{J} = \frac{c_1}{m_1}{\rm e}^{m_1 t} + \frac{c_2}{m_2}{\rm e}^{m_2 t} - \frac{c_1}{m_1} - \frac{c_2}{m_2}, \tag{A.3a}$$

for $D = 0$

$$\frac{\Gamma}{J} = \frac{c_1 m_1 - c_2 + c_2 m_1 t}{m_1^2}{\rm e}^{m_1 t} - \frac{c_1 m_1 - c_2}{m_1^2}, \tag{A.3b}$$

for $D < 0$

$$\frac{\Gamma}{J} = \frac{c_1 p - c_2 q}{p^2 + q^2}({\rm e}^{pt}\cos qt - 1) + \frac{c_1 q + c_2 p}{p^2 + q^2}{\rm e}^{pt}\sin qt, \tag{A.3c}$$

where the constants are the same as in equation (A.2).

A.2 n-Step model

The adsorption of polymers, but of course also of other molecules, can be addressed by assuming that the molecule can exist in $n + 1$ different states, either in solution or at the interface. It is then possible to use first order reaction kinetics to describe the adsorption process. The differential equations for the adsorbed amounts of the different states take the following general form:

$$\dot{\Gamma}_j = A_{jk}\Gamma_k + J_j. \tag{A.4}$$

We denote the eigenvalues and eigenvectors of the $m \times m$ matrix A_{jk} by λ_j and v_{jk}, respectively. In the case all eigenvalues are distinct, solution of the homogeneous equation $\dot{\Gamma}_j^{\rm h} = A_{jk}\Gamma_k^{\rm h}$ gives

$$\Gamma_{jk}^{\rm h} = v_{jk}{\rm e}^{\lambda_j t}, \tag{A.5}$$

arriving at the general solution $\Gamma_j^{\rm h} = C_k\Gamma_{kj}^{\rm h}$, where C_k is a constant vector. To find a particular solution we apply the technique of variation of constants, i.e., we put

$$\Gamma_j^{\rm p} = B_k(t)\Gamma_{kj}^{\rm h}, \tag{A.6}$$

after which it is easy to show that

$$\dot{B}_k\Gamma_{kj}^{\rm h} = J_j. \tag{A.7}$$

Taking a single exponential function for B_j meets the set requirements. We take $B_j = \frac{b_j}{\lambda_j}{\rm e}^{-\lambda_j t}$. The full solution of equation (A.4) then is

$$\begin{aligned}\Gamma_j &= \Gamma_j^{\rm h} + \Gamma_j^{\rm p} \\ &= (C_k + B_k)\Gamma_{kj}^{\rm h}.\end{aligned} \tag{A.8}$$

Using the boundary condition $\Gamma_j(0) = \Gamma_j^0$ and equation (A.7) we are able to calculate the introduced constants b_j and c_j. In the case we have a set of two differential equations, as is the case throughout this paper, then

$$b_1 = \frac{j_1 v_{22} - j_2 v_{21}}{v_{12}v_{21} - v_{11}v_{22}}, \tag{A.9a}$$

$$b_2 = \frac{j_2 v_{11} - j_1 v_{12}}{v_{12}v_{21} - v_{11}v_{22}}, \tag{A.9b}$$

$$c_1 = -\frac{b_1}{\lambda_1} - \frac{\Gamma_1^0 v_{22} - \Gamma_2^0 v_{21}}{v_{12}v_{21} - v_{11}v_{22}}, \tag{A.9c}$$

$$c_2 = -\frac{b_2}{\lambda_2} - \frac{\Gamma_2^0 v_{11} - \Gamma_1^0 v_{12}}{v_{12}v_{21} - v_{11}v_{22}}, \tag{A.9d}$$

where $\lambda_1 \neq \lambda_2$.

References

1. G.J. Fleer, M.A. Cohen Stuart, J.M.H.M. Scheutjens, T. Cosgrove, B. Vincent, *Polymers at interfaces* (Chapman & Hall, London, 1993).
2. E. Pefferkorn, A. Elaissari, J. Colloid Interface Sci. **138**, 187–194 (1990).
3. A. Elaissari, E. Pefferkorn, J. Colloid Interface Sci. **143**, 85–91 (1991).
4. H.M. Schneider, P. Frantz, S. Granick, Langmuir **12**, 994–996 (1996).
5. M.C.P. van Eijk, M.A. Cohen Stuart, Langmuir **13**, 5447–5450 (1997).
6. J. Buijs, P.A.W. van den Berg, J.W.Th. Lichtenbelt, W. Norde, J. Lyklema, J. Colloid Interface Sci. **178**, 594–605 (1996).
7. J.C. Dijt, M.A. Cohen Stuart, G.J. Fleer, Macromolecules **27**, 3219–3228 (1994).
8. A.N. Semenov, J.-F. Joanny, J. Phys. II France **5**, 859–876 (1995).
9. T. Dąbroś, T.G.M. van de Ven, Colloid Polym Sci. **261**, 694–707 (1983).
10. J.C. Dijt, M.A. Cohen Stuart, J.E. Hofman, G.J. Fleer, Colloids Surf. **51**, 141–158 (1990).
11. J.C. Dijt, M.A. Cohen Stuart, G.J. Fleer, Adv. Colloid Interface Sci. **50**, 79–101 (1994).
12. D.J.M. Bergink-Martens, H.J. Bos, A. Prins, and B.C. Schulte, J. Colloid Interface Sci. **138**, 1–9 (1990).
13. T. Dąbroś, Z. Adamczyk, Chem. Eng. Sci. **34**, 1041–1049 (1979).